

# On-Demand Formation of Supported Lipid Membrane Arrays by Trehalose-Assisted Vesicle Delivery for SPR Imaging

Samuel S. Hinman,<sup>†</sup> Charles J. Ruiz,<sup>‡</sup> Georgia Drakakaki,<sup>§</sup> Thomas E. Wilkop,<sup>\*,§</sup> and Quan Cheng<sup>\*,†,‡</sup>

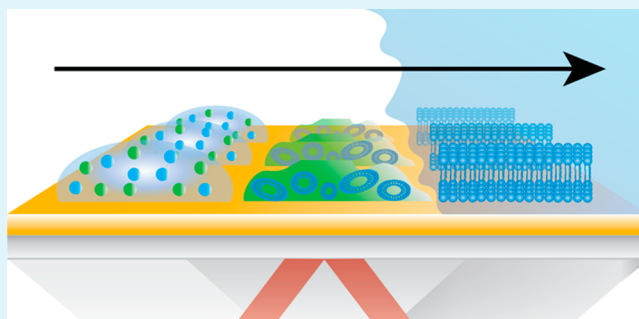
<sup>†</sup>Environmental Toxicology and <sup>‡</sup>Department of Chemistry, University of California, Riverside, Riverside, California 92521, United States

<sup>§</sup>Department of Plant Sciences, University of California, Davis, Davis, California 95616, United States

## Supporting Information

**ABSTRACT:** The fabrication of large-scale, solid-supported lipid bilayer (SLB) arrays has traditionally been an arduous and complex task, primarily due to the need to maintain SLBs within an aqueous environment. In this work, we demonstrate the use of trehalose vitrified phospholipid vesicles that facilitate on-demand generation of microarrays, allowing each element a unique composition, for the label-free and high-throughput analysis of biomolecular interactions by SPR imaging (SPRi). Small, unilamellar vesicles (SUVs) are suspended in trehalose, deposited in a spatially defined manner, with the trehalose vitrifying on either hydrophilic or hydrophobic SPR substrates. SLBs are subsequently spontaneously formed on-demand simply by in situ hydration of the array in the SPR instrument flow cell. The resulting SLBs exhibit high lateral mobility, characteristic of fluidic cellular lipid membranes, and preserve the biological function of embedded cell membrane receptors, as indicated by SPR affinity measurements. Independent fluorescence and SPR imaging studies show that the individual SLBs stay localized at the area of deposition, without any encapsulating matrix, confining coral, or boundaries. The introduced methodology allows individually addressable SLB arrays to be analyzed with excellent label-free sensitivity in a real-time, high-throughput manner. Various protein–ganglioside interactions have been selected as a model system to illustrate discrimination of strong and weak binding responses in SPRi sensorgrams. This methodology has been applied toward generating hybrid bilayer membranes on hydrophobic SPR substrates, demonstrating its versatility toward a range of surfaces and membrane geometries. The stability of the fabricated arrays, over medium to long storage periods, was evaluated and found to be good. The highly efficient and easily scalable nature of the method has the potential to be applied to a variety of label-free sensing platforms requiring lipid membranes for high-throughput analysis of their properties and constituents.

**KEYWORDS:** SLB, HBM, SPR, SPR imaging, devitrification, microarray



## ■ INTRODUCTION

The cell membrane is a fundamental structure of living organisms, separating exterior and interior content, with embedded receptors and structures facilitating communication and regulated active and passive material exchange.<sup>1</sup> This interface principally serves as a selective barrier for a range of exogenous materials, including ions, metabolites, growth factors, and toxins. As a plethora of recognition sites in the membrane translate biotic and abiotic environmental stimuli across the membrane, these are primary targets in studies toward a better understanding of signaling pathways and how biological responses are effected on the cellular level.<sup>2</sup> Supported lipid bilayer (SLB) systems, typically formed on glass<sup>3</sup> or PDMS,<sup>4</sup> have proven to be a convenient platform for these studies, as the isolated lipid environment eliminates complexities and interferences from other cellular activities. These SLBs are easily tunable with a broad spectrum of compositional complexities ranging from single phospholipids to mixtures of lipids with embedded proteins and natural

receptors.<sup>5,6</sup> Thus far, SLB systems have been used for a variety of applications, including gaining insight into biophysical processes,<sup>7,8</sup> enhancing drug delivery through incorporation of synthetic receptors,<sup>9</sup> and designing sensors that bind molecules to their natural targets.<sup>10–12</sup>

Despite the potential and flexibility of SLBs, microarray applications of these systems have been scant. This is in large part due to the complexity and limited scalability of generating and maintaining SLBs in an aqueous environment in a way that ensures membrane integrity and unaltered activity of embedded components. Currently, common methods of creating patterned lipid bilayer microarrays include utilizing lipid corrals,<sup>13</sup> utilizing noncontact printing through confined films,<sup>14</sup> and injecting single-composition vesicle suspensions over multielement array substrates.<sup>15</sup> Each of these methods

**Received:** May 1, 2015

**Accepted:** July 20, 2015

**Published:** July 20, 2015

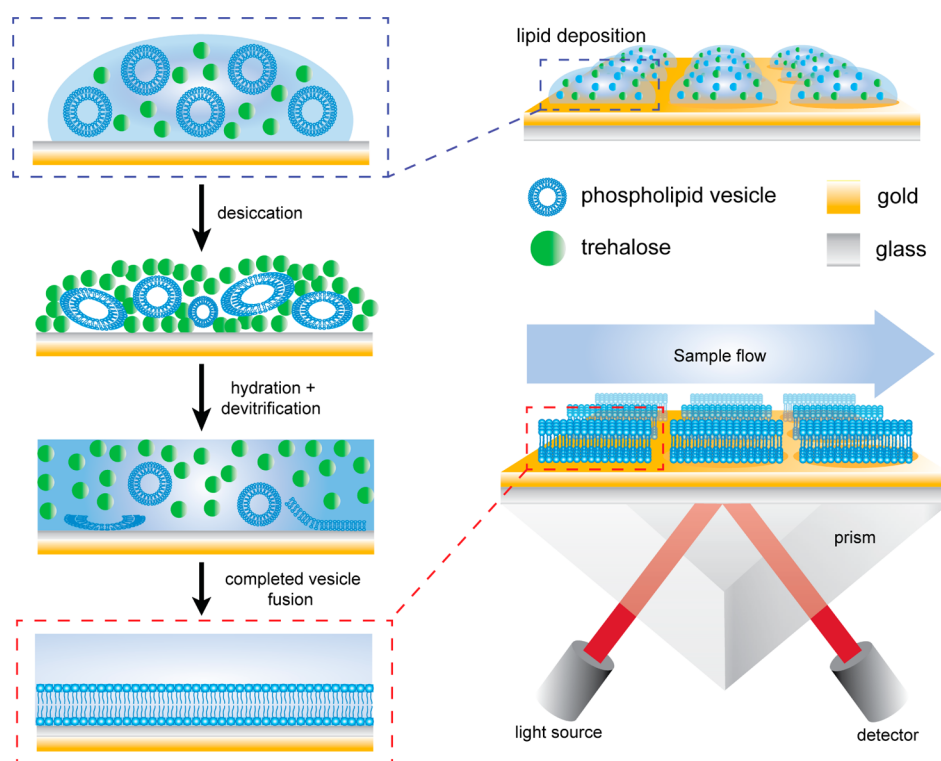


**Figure 1.** Schematic diagram showing the process of vesicle deposition, desiccation, and devitrification upon hydration of the trehalose matrix on the modified SPR sensor chips. Each SPR chip is modified with ca. 10 nm of silica, applied by plasma-enhanced chemical vapor deposition to increase hydrophilicity and provide a fusogenic surface for the SUVs. The devitrification process releasing the SUVs takes place in the SPR flow cell environment.

crucially depends on constant hydration of the fabricated array, as exposure to air results in a loss of structural integrity of the SLB. This translates to required on site fabrication of SLBs, with severe limits for even short-term storage and transport of SLB array substrates, facts that make commercialization and widespread adaption very challenging. However, a unique fabrication method was recently introduced that allows for the spatially defined deposition of matrix encapsulated lipid vesicles, followed by on-demand formation of solid-supported lipid bilayers once hydrated.<sup>16</sup> With addition of a low molecular weight, nonreducing disaccharide, trehalose, to preformed vesicle suspensions, a strategy that mimics the natural preservation mechanisms encountered in drought-tolerant and anhydrobiotic organisms,<sup>17,18</sup> vesicles remain intact during the vitrification of trehalose. Hydration leads to a devitrification of trehalose, removal of the sugar, and a concurrent release of the vesicles followed by their fusion into SLBs on fusogenic surfaces. Resulting lipid bilayers on glass were studied by fluorescence microscopy, and were shown having fluidity comparable to conventional SLBs, as well as being capable of maintaining embedded ligands and receptors in their active state throughout the trehalose vitrification and devitrification processes.<sup>16</sup>

Compared to fluorescence, label-free analytical methods such as surface plasmon resonance (SPR) allow for the characterization of molecular interactions in a highly efficient fashion without extra labeling or tagging steps, thereby eliminating potential interference and labor.<sup>19</sup> SPR assays have successfully been applied toward studying a large variety of chemical and biological samples,<sup>20</sup> and are user-friendly enough to be conducted in clinical settings.<sup>21</sup> Many early studies utilizing SPR for investigating lipid membrane systems made use of

hybrid bilayer membranes,<sup>10,22</sup> where the hydrophobic tails of phospholipids adsorb to long-chain alkanethiol monolayers assembled on gold substrates. In previous work, we demonstrated that, by creating nanoscale layers of glass on gold surfaces,<sup>23</sup> formation and characterization of stable bilayer membranes is also possible for SPR. Recently, a number of high-performance SPR imaging (SPRi) substrates have been developed that allow for ultrasensitive screenings of SLB systems in a high-throughput manner.<sup>24,25</sup> These substrates featured thin coatings of silica, applied through advanced cleanroom techniques, attenuated background evanescent fields to yield higher dynamic response ranges, and allowed for the detection of proteinaceous toxins binding to receptor-containing SLBs at low nanomolar concentrations.

In this work, we report an approach that combines trehalose-assisted phospholipid vesicle deposition with SPRi for on-demand and label-free analysis of biomolecular interactions in an arrayed SLB system. Vesicle suspensions in trehalose were deposited on ultrathin (10 nm) layers of engineered glass deposited on gold substrates, desiccated, and directly used for analytical characterization once rehydrated (Figure 1). Lateral mobility properties of traditionally formed bilayers and those that stem from rehydrated lipids released from trehalose were compared on a variety of substrate surfaces, including Au/SiO<sub>2</sub> glass coverslips and alkanethiol-modified Au. After empirically optimizing the flow rate conditions for the rehydration within the SPR flow cell, we studied the behavior of the generated lipid membranes by SPR in terms of the effective refractive index changes compared to traditionally formed membranes. Furthermore, affinity studies were carried out with cell membrane receptors, namely, gangliosides GM1, GM2, and GM3, in which the response signals for the binding of cholera

toxin to differently prepared bilayers were found to be virtually identical. SPRi experiments showed no crosstalk between adjacent array elements. Individual binding responses of multiple monosialogangliosides across a multielement array were compared and exhibited excellent coherence, underscoring the utility of this versatile methodology for large-scale arrays. In addition to the fluid SLB arrays on Au/SiO<sub>2</sub> substrates, we also show on-demand bilayer formation on hydrophobic surfaces resulting in hybrid bilayers and their characterization.

## ■ EXPERIMENTAL SECTION

**Materials and Reagents.** Cholera toxin (CT) from *Vibrio cholera*, Triton X-100, 1-octadecanethiol (98%), and *n*-octadecyltrichlorosilane (OTS, 90+%) were from Sigma-Aldrich (St. Louis, MO). Trehalose was from Swanson Health Products (Fargo, ND).

1-Palmitoyl-2-oleoyl-*sn*-glycero-3-phosphocholine (POPC) and 1-palmitoyl-2-{6-[(7-nitro-2-1,3-benzoxadiazol-4-yl)amino]hexanoyl}-*sn*-glycero-3-phosphocholine (NBD-PC) were from Avanti Polar Lipids (Alabaster, AL). Monosialoganglioside GM1 (NH<sub>4</sub><sup>+</sup> salt) and monosialoganglioside GM2 (NH<sub>4</sub><sup>+</sup> salt) were from Matreya (Pleasant Gap, PA). Monosialoganglioside GM3 was from EMD Biosciences (La Jolla, CA). BK-7 glass substrates were from Corning (Painted Post, NY). Chromium and gold used for electron-beam evaporation were acquired as pellets of 99.99% purity from Kurt J. Lesker (Jefferson Hills, PA).

**Vesicle Preparation.** An appropriate amount of lipid stock solution containing 95% (w/w) POPC and 5% (w/w) monosialoganglioside (GM1, GM2, or GM3) in chloroform was dried in a glass vial under nitrogen to form a thin lipid film. The vial containing lipids was then placed in a vacuum desiccator for at least 2 h to remove any residual solvent. The dried lipids were resuspended in 1× PBS (10 mM Na<sub>2</sub>HPO<sub>4</sub>, 1.8 mM KH<sub>2</sub>PO<sub>4</sub>, 137 mM NaCl, 2.7 mM KCl, pH 7.4) to a lipid concentration of 2.0 mg/mL. After vigorous vortexing to remove all lipid remnants from the vial wall, the solution was probe sonicated for 20 min. The resuspended lipids were then centrifuged at 8000 rpm for 15 min to remove titanium particles from the sonicator probe tip. Thereafter, the supernatant was extruded through a polycarbonate filter (100 nm) to produce small, unilamellar vesicles (SUVs) of uniform size. If the vesicles were suspended in trehalose, the solution was diluted to a final concentration of 1.0 mg/mL PC in 50 mM trehalose using a trehalose/1× PBS mixture. If not, the solution was diluted to 1.0 mg/mL PC using 1× PBS. For fluorescence analysis, the vesicle preparation followed the same procedure with the addition of 2% (w/w) NBD-PC. All vesicle suspensions were applied within a week and stored at 4 °C before use.

**SPR Chip Fabrication.** SPR and SPRi chips were fabricated using BK-7 glass microscope slides. First, BK-7 substrates were cleaned using boiling piranha solution (3:1 H<sub>2</sub>SO<sub>4</sub>/30% H<sub>2</sub>O<sub>2</sub>) for 30 min, followed by rinsing with DI water and drying under compressed air. For conventional SPR chips, 2.0 nm of chromium (0.5 Å/s) followed by 46.0 nm of gold (1.0 Å/s) was deposited using electron beam evaporation (Temescal, Berkeley, CA) at 5 × 10<sup>-6</sup> Torr. To obtain a hydrophilic surface for lipid bilayer formation, 10 nm of SiO<sub>2</sub> was deposited on top of the gold layer using plasma enhanced chemical vapor deposition (PECVD) with a Unaxis Plasmatherm 790 system (Santa Clara, CA).

High-performance gold well SPRi chips were fabricated using previously developed methods<sup>24</sup> (Figure S1, Supporting Information). A 2.0 nm layer of chromium and 51.0 nm of gold were deposited using electron beam evaporation on cleaned BK-7 glass substrates using the above protocol. The surface was then rendered hydrophilic with 10 nm coating of SiO<sub>2</sub> deposited by PECVD. Subsequently, photoresist AZ5214E was spin coated on the gold/SiO<sub>2</sub> at 4000 rpm, and the surface was patterned into mesas representing the final array spots using standard photolithography methods. After a second electron beam evaporation of 100.0 nm of gold, the photoresist was lifted off

with acetone, leaving an elevated gold grid behind, defining the array elements on the SiO<sub>2</sub>.

Prior to use, all SPR substrates were thoroughly rinsed alternately with DI water, isopropanol, and DI water and then dried in a stream of nitrogen. The hydrophilicity of SiO<sub>2</sub> coated chips was additionally increased by exposure to an oxygen plasma for 60 s using a Harrick PDC-32G plasma cleaner (Harrick Plasma, Ithaca, NY).

**SPR and SPRi Instrumentation.** A dual-channel SPR spectrometer, NanoSPR5-321 (NanoSPR, Chicago, IL), with a GaAs semiconductor laser light source ( $\lambda = 670$  nm) was used for all spectroscopic SPR measurements. The device was equipped with a manufacturer-supplied high-refractive index prism ( $n = 1.61$ ) and a 30  $\mu$ L flow cell. Surface interactions at the gold interface were monitored using the resonance angle tracking mode.

A detailed description of the SPR imaging instrumentation setup has been provided in previous work.<sup>26</sup> In brief, each BK7 substrate coated with gold well arrays was mounted on an optical stage containing a 300  $\mu$ L flow cell. Each array was put in contact with an equilateral SF2 prism ( $n = 1.616$ ) using refractive index matching fluid ( $n = 1.616$ , Cargille Laboratories, Cedar Grove, NJ). The optical stage was fixed on a goniometer that allows manual selection of the incident light angle. A incoherent light source (LED,  $\lambda = 648$  nm) was used for SPR excitation, and the reflected images were captured by a cooled 12-bit CCD camera, Retiga 1300 (QImaging, Surrey, BC, Canada) with a resolution of 1.3 MP (1280 × 1024 pixels) and 6.7  $\mu$ m × 6.7  $\mu$ m pixel size. Injections of sample solutions into the flow cell were monitored in real time by recording changes in the reflectance every 300 ms inside the gold array wells and for reference purpose on the surroundings. Sensorgrams were obtained by averaging reflected light intensity over each array element using a home-built LabView program. Difference images were obtained by subtracting images collected with p-polarized from those recorded with s-polarized light.

**Desiccation of Vesicle Suspensions.** An appropriate amount of preformed SUVs in 50 mM trehalose and 1× PBS (50  $\mu$ L for SPR channels, 20  $\mu$ L for fluorescence wells, 200 nL for SPRi array spots) was deposited on the chosen substrate surface and dried overnight in a vacuum desiccator; substrates were typically left under vacuum until use. In the case of the long-term storage assessment, substrates were moved from vacuum to ambient conditions after 12 h.

**Devitrification of Trehalose Coatings.** Both the SPR and SPRi setups employ home-built fluidic systems at ambient temperature (~23 °C), with 1× PBS used as the running buffer set to a flow rate of 6 mL/h unless otherwise noted. The substrates with trehalose suspended vesicles were placed directly into the SPR or SPRi instruments and rehydrated within the flow cell environment. Once a stable signal was obtained, indicating completion of the membrane formation and removal of excess material, the lipid bilayers were used for analytical studies.

**Fluorescence Microscopy and FRAP Analysis.** Fluidity of membranes from traditional fusion of POPC vesicles and those from hydrated trehalose encapsulated POPC vesicles on different surfaces was examined using fluorescence recovery after photobleaching (FRAP). Supported lipid bilayers were formed on bare glass coverslips (Fisher Scientific, Pittsburgh, PA), glass coverslips covered with 10 nm of SiO<sub>2</sub>, and C18-modified glass coverslips. For the trehalose derived membranes, 20  $\mu$ L of 2% (w/w) NBD-PC/98% (w/w) POPC in 50 mM trehalose and 1× PBS was deposited into 4.5 mm PDMS wells on top of the glass/modified Au substrates. Following an overnight dehydration in vacuum the vesicle suspension was rehydrated in 1× PBS buffer *in situ* the following day and rinsed thoroughly with DI water to remove unfused vesicles. For traditional membranes, 20  $\mu$ L of 2% (w/w) NBD-PC/98% (w/w) POPC in 1× PBS was deposited into the PDMS wells and allowed to incubate for 1 h prior to rinsing with water. To assist with the identification of the focal plane for the bilayer under the microscope, a peripheral scratch on the membrane was made and used. Fluorescence microscopy was carried out on an inverted Leica TCS SP5 II (Leica Microsystems, Buffalo Point, IL) using the 488 nm Argon laser line and a 40× (NA 1.1) objective. Photobleaching at 1.5 mW for 500 ms and fluorescence recovery

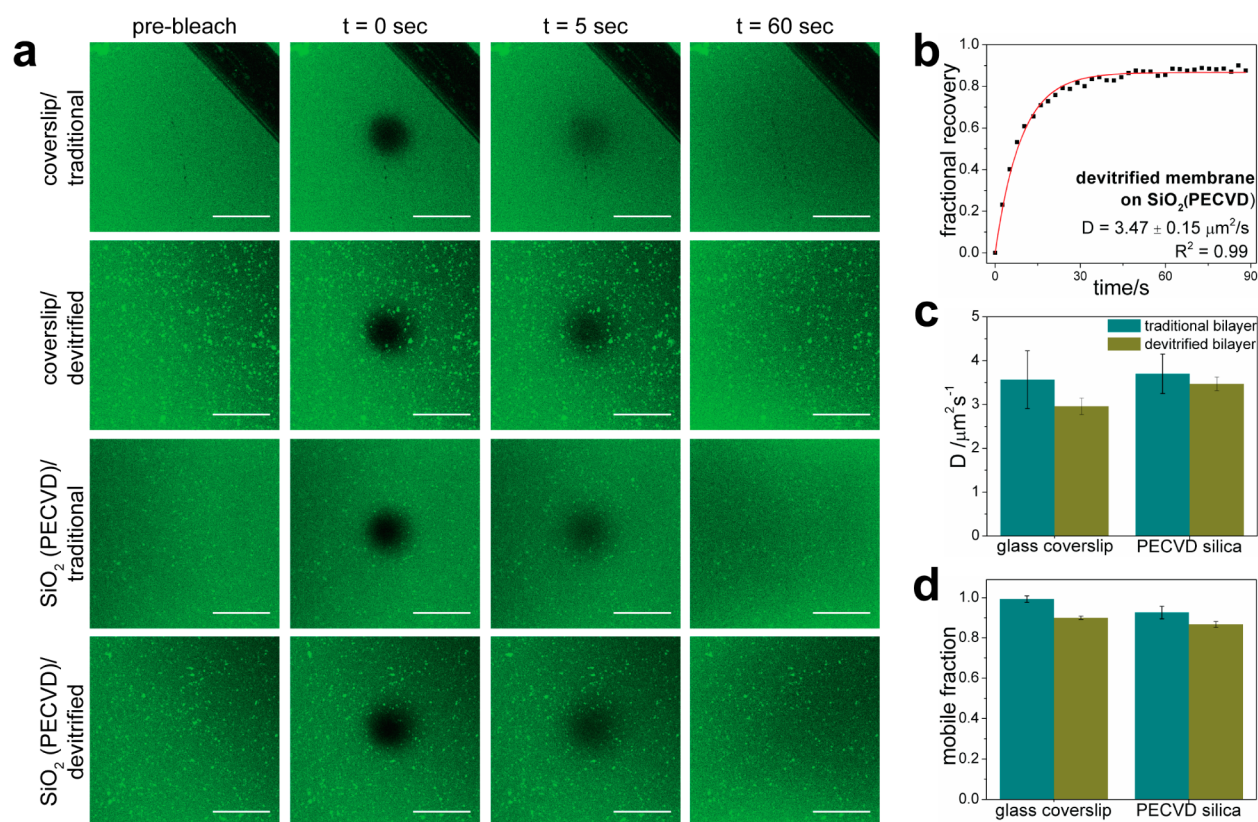


**Figure 2.** FRAP analysis of supported lipid bilayers formed using direct, traditional vesicle fusion and trehalose assisted deposition methods on microscope coverslips and SiO<sub>2</sub>-modified SPR surfaces. Calculated values are the result of  $N = 3$  experiments. (a) Fluorescence microscopy images showing bleaching and recovery of fluorescence due to redistribution of lipids over time. Scale bars represent 20  $\mu\text{m}$ . (b) FRAP recovery curve of the devitrified membrane on modified SPR surface. (c) Diffusion coefficients. (d) Mobile fractions.

monitoring were set up and performed using the LAS AF software package (Leica Microsystems, Buffalo Point, IL).

The methods of Axelrod and Soumpasis were applied to determine mobile fractions, half-time recovery values, and diffusion coefficients.<sup>27,28</sup> First, the fluorescence intensity of each bleach spot was normalized over a background area of the same size to account for background photobleaching. This normalized value ( $F_n$ ) was then used within the following formula to obtain the FRAP ratio ( $F_{\text{FRAP}}$ ), with  $F_0$  being the normalized intensity of the bleached area immediately after bleaching.

$$F_{\text{FRAP}} = (F_n - F_0)/(1 - F_0) \quad (1)$$

Thereafter,  $F_{\text{FRAP}}$  was plotted against time and fitted to a first order exponential function. The diffusion coefficient was then calculated using the diffusion eq 2, with  $D$  being the diffusion coefficient,  $\omega$  the full width at half-maximum of the focused laser's Gaussian profile,  $t_{1/2}$  the half-time recovery obtained from the exponential fit, and  $\gamma$  a correction factor accounting for the laser beam geometry.

$$D = (\omega^2/4t_{1/2})\gamma \quad (2)$$

## RESULTS AND DISCUSSION

**Diffusion Kinetics of Devitrified Membranes on SPR Surfaces.** Glass has been used as a standard substrate for SLB studies, as it offers robust solid support for membrane formation from vesicle fusion, and the resulting membranes exhibit fluidic properties comparable to those of native cell membranes.<sup>29</sup> In order to be compatible with SPR detection, while maintaining acceptable sensitivity, glass layers must be as thin as possible, ideally on the nanometer scale, since the SPR evanescent field decays exponentially with distance from the

gold surface. As noted in previous work,<sup>23,30</sup> the layer-by-layer assembly of polyelectrolytes and sodium silicate followed by high-temperature calcination is an effective and low-cost way to produce glassy silicate films of uniform, nanoscale thickness. Here we chose to explore membrane formation on SPR substrates on which silica (SiO<sub>2</sub>) is deposited by plasma-enhanced chemical vapor deposition (PECVD). This method offers the advantage of short process times (under 10 min) and remarkably smooth surfaces, which benefits lipid bilayer fluidity and minimizes optical scattering. Previous studies<sup>31,32</sup> have established that these surfaces are characterized by low surface roughness values (rms <1.5 nm) and high stability in buffer conditions compared to silica deposited using thermal evaporation.<sup>33</sup> However, the properties of SLBs on PECVD grown silica have not been fully investigated to determine if their diffusion kinetics match those on other glass-supported bilayers.

Fluorescence recovery after photobleaching (FRAP) was performed to verify that the bilayers formed by traditional vesicle injection and through trehalose assisted delivery methods on glass coverslips (standard solid support) and silica surfaces deposited using PECVD (Figure 2) were contiguous, uniform, and fluidic. The fluorescence images (Figure 2a) show that all bilayers uniformly cover their respective surfaces, without defects or voids that would be indicative of a lack of membrane fusion. One minor difference to be noted when comparing the traditional versus devitrified membranes is that membranes originating from vesicles released from the devitrified trehalose showed a stronger abundance of small, higher fluorescence intensity patches across the membrane

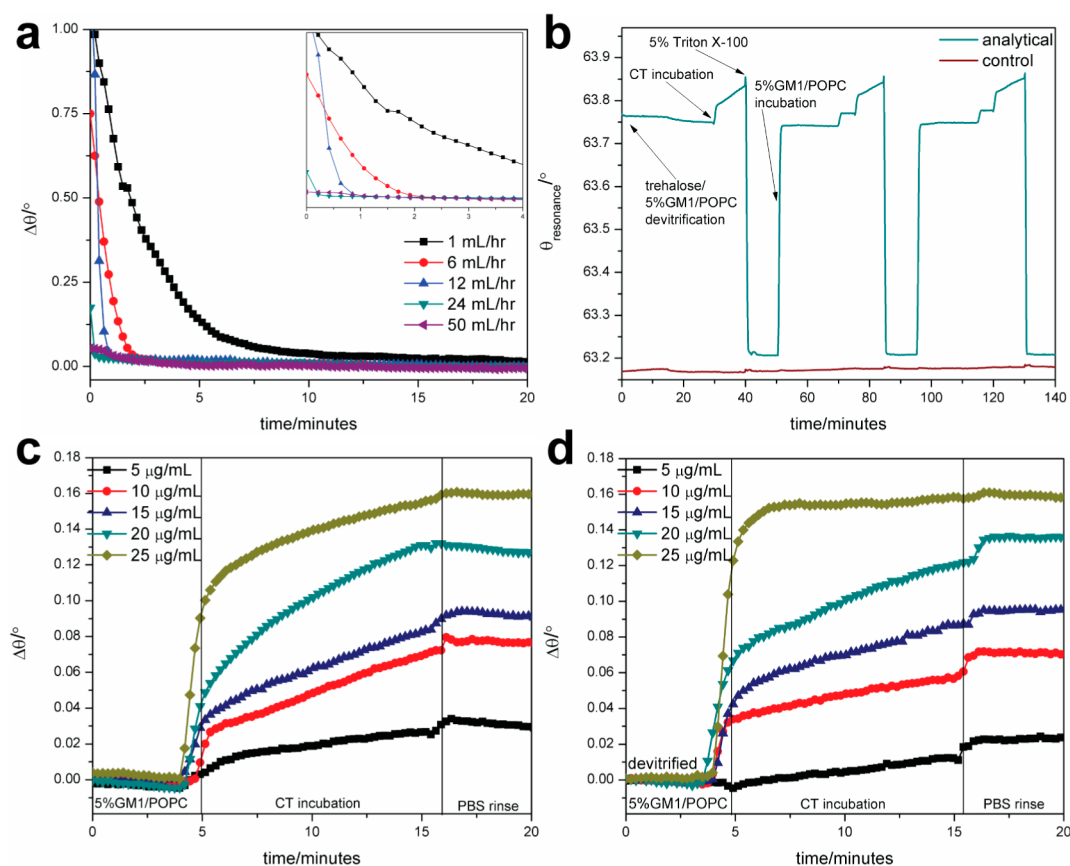


**Figure 3.** SPR studies of vesicle fusion upon devitrification of trehalose and preservation of embedded cargo activity. (a) Flow rate effects on devitrification of trehalose, release of SUVs, and formation of supported lipid bilayers. (b) Formation of supported lipid bilayer from trehalose released SUVs containing GM1 and subsequent CT binding response, followed by a comparative study on the identical chip of the same system generated by traditional vesicle fusion, showing excellent agreement. (c) Responses of membranes formed by vesicle injection methods to cholera toxin injections. (d) Responses of membranes formed by vesicle preservation and devitrification methods to cholera toxin injections.

surface on the  $\text{SiO}_2$ -covered SPR substrates. This may be attributed to the rehydrating conditions used for the devitrification of trehalose with some rehydrated lipids only partially fusing and remaining as aggregates at the glass/lipid interface. However, this only appears to have a minimal impact on the diffusion kinetics of lipids within the bilayer, as seen when comparing the fractional recovery profiles and their associated kinetic values (Figure 2b–d, also see Figure S2, Supporting Information). It should be noted that the fractional recovery profile for membranes from trehalose released vesicles on PECVD silica is relatively smooth and fits the lateral diffusion curve well ( $R^2 = 0.99$ ), strongly indicating a natural and uniform bilayer (Figure 2b). While the lateral mobilities of traditional membranes (Figure 2b) are slightly higher, all diffusion coefficients ( $D$ 's) are between 2 and 4  $\mu\text{m}^2/\text{s}$  (Figure 2c). The slightly lower lateral mobilities of trehalose formed membranes may be due to trace amounts of trehalose remaining under the bilayer, affecting the short-range interactions between the lipids and glass support. However, all values still compare favorably with previous studies of phosphatidylcholine based SLBs on glass surfaces, where diffusion coefficients ranged between 1 and 4  $\mu\text{m}^2/\text{s}$ .<sup>29</sup>

Another interesting observation is that mobile fractions ( $\beta$ 's) differ slightly when comparing membranes on glass coverslips and silica deposited using PECVD (Figure 2d). In general, mobile fractions were higher for bilayers on glass coverslips, 99% and 90% for traditional and devitrified trehalose,

respectively, than for bilayers on the PECVD surface, with 92% and 86%, respectively. Lower mobile fractions have previously been attributed to higher surface roughness of the underlying material,<sup>34</sup> though PECVD surfaces are known to be quite smooth.<sup>31,32</sup> These lower mobile fractions are more likely to be due to the different levels of hydrogen bonding observed in PECVD grown dielectrics, thereby changing the affinity for phospholipids at the surface,<sup>35</sup> or to remnants of trehalose remaining under the bilayer. Nevertheless, all mobile fraction values are quite high, and taken together with the high diffusion coefficients and continuous fluorescence signal, the data suggests that a fluid and natural membrane is formed using trehalose preserved vesicles on PECVD grown silica, resulting in an SLB that is capable of full biological functionality<sup>36,37</sup> and suitable for SPR imaging and spectroscopic studies.

**SPR Monitoring of SLB Formation from Trehalose Encapsulated Vesicles and Toxin Binding.** SPR has been established as a universal tool for monitoring interactions at membrane interfaces,<sup>10,15</sup> as the probing evanescent field of SPR is most sensitive directly near the gold surface on which lipid bilayers are supported. Vesicles were deposited by spotting an appropriate amount of small, unilamellar vesicles (SUVs) suspended in 50 mM trehalose onto the silica coated SPR chips, followed by drying overnight in vacuum. These SUVs in vitrified trehalose were rehydrated in the SPR flow cell, and the trehalose devitrification and vesicle fusion processes leading to on-demand lipid bilayer formation were monitored in real time.

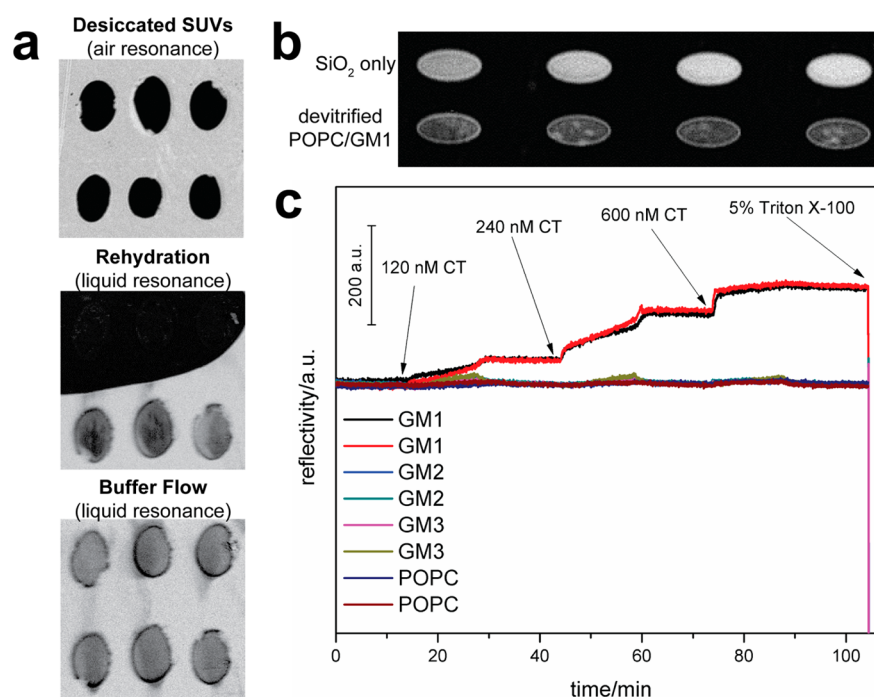


**Figure 4.** SPR imaging study of membrane arrays formed using trehalose deposited and preserved vesicles. (a) Spatial confinement of lipids before, during, and after rehydration. The middle image exhibits the buffer front. (b) SPR difference image comparing bare silica surface and membrane covered surface. (c) SPR imaging sensorgrams comparing cholera toxin binding to SLBs of various compositions on the same SPR imaging substrate.

Rehydration of the SUVs was carried out over a range of flow rates, set between 1 and 50 mL/h (Figure 3a). There are a number of processes occurring at the substrate surface during rehydration, which include devitrification of trehalose, diffusion of trehalose into solution, diffusion of SUVs into solution, and fusion of SUVs to the adjacent substrate surface.<sup>16</sup> Given the flow cell arrangement employed in our studies, the flow rate is a vital parameter to ensure that upon devitrification of the trehalose the release of vesicles ensures formation of a contiguous membrane before mass transport away from the surface leads to SUV depletion. For lower flow rates in the range 1–6 mL/h, a substantial amount of time was required for SPR sensorgrams to reach a flat baseline, which we interpret as a stable bilayer. It is possible that SUVs remain adsorbed to the bilayer interface and are only gradually removed in the flowing buffer. Given the high solubility of trehalose in water, it is unlikely that gradual trehalose removal can fully account for the observed behavior. This was confirmed by a control where only trehalose was desiccated and rehydrated, resulting in only a partial resonance angle decrease compared to when both vesicles and trehalose were rehydrated (Figure S3, Supporting Information). The former is in agreement with the observation of small phospholipid aggregates in the fluorescence images (Figure 2a). Higher flow rates between 12 and 50 mL/h allowed for complete vesicle fusion and excess removal without an extended equilibration period; therefore, all further assays used an initial rapid flow rate of 24 mL/h for rehydration, followed by a lower flow rate of 6 mL/h during affinity measurements to minimize laminar shear forces on the bilayer.

The binding properties of embedded receptors in the SLBs formed on-demand by this method were compared to SLBs containing the same receptors but formed by the traditional vesicle injection method on the identical substrate. For this evaluation, it was first established that SLBs originating from the two methods yield similar membrane thicknesses. For this,

equilibrated SLBs formed with trehalose assistance on the SPR chips were stripped away with buffer containing 5% Triton X-100, and new SLBs were generated by incubating the identical substrate with a fresh SUV suspension. The observed resonance angle shifts of the SPR chip match precisely for both methods each time a new lipid bilayer is formed on the surface (Figure 3b). SPR is a refractive index sensitive method, in which the observed signal change for SLBs is determined by their unique bulk refractive index and geometry, and in this case the SLB thickness;<sup>19</sup> here, the observed similarities in resonance angles between the two types of bilayers strongly suggest that their thicknesses and effective masses are identical. The above evaluation strategy was also explored in the context of biointeraction analyses, using the model system of cholera toxin (CT) binding to the membrane-bound GM1 receptor. Over a range of concentrations, the response signals at equilibrium for CT-GM1 interactions are very similar (Figure 3c,d), indicating that, throughout the vitrification, rehydration, and fusion processes, receptors embedded in the preserved vesicles retain biological activity and respective ligand affinities comparable to those not undergoing desiccation and rehydration. This was further evaluated over a period of 4 weeks, in which measurements of CT binding to different POPC/GM1 membranes, deposited at the same time, were taken at regular intervals. Response signals remained nearly unchanged over the 28 days, exhibiting only a 4.3% relative standard deviation at a CT concentration of 20  $\mu\text{g}/\text{mL}$  (Figure S4, Supporting Information). It should be noted that each of these substrates were left in ambient conditions over the month, not requiring continuous desiccation or refrigeration. Given that this involves humidity and temperature fluctuations, the sub-5% standard deviation in the response is very good but could possibly be improved in a more controlled environment. Preservation of biological function during medium and long-

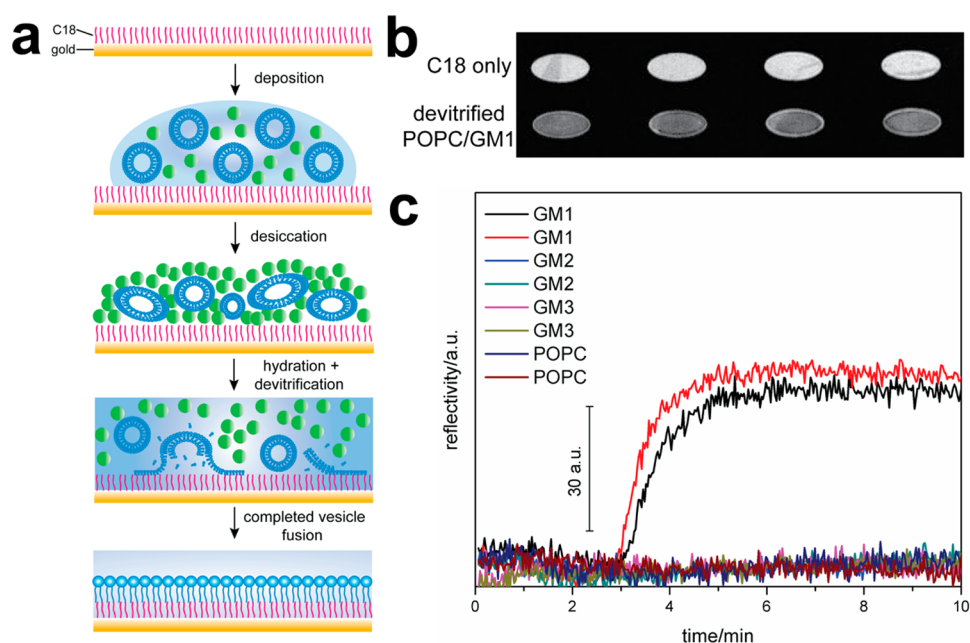


**Figure 5.** Hybrid bilayer membrane formation on SPR substrates using trehalose assisted vesicle delivery. (a) Scheme of deposition, desiccation, and hydration on hydrophobic rendered SPR surface. (b) SPR difference image comparing bare C18 surface and membrane-covered surface. (c) SPR imaging sensorgrams comparing cholera toxin binding to HBMs of various compositions on the same SPR imaging substrate.

term storage is essential for a practical, expanded deployment of this methodology.

**SPR Imaging of Multielement SLB Arrays.** SPR imaging is a powerful tool for real-time and label-free microarray analysis, expanding the throughput of assays and minimizing artifacts from sequential measurements. Analyzing SLB microarrays with varying bilayer compositions remains a challenging task, mainly due to the requirement of maintaining constant hydration of the substrate during the arraying, handling, and assaying processes. One option to generate membrane arrays of varying compositions is to utilize multiple microfluidic channels during the formation and analysis of supported lipid bilayers.<sup>38</sup> While this approach is promising for analyzing multiple “lanes” in real-time, fluidics with an open chamber design offer the advantage of exposing all array elements to the same analyte and flow conditions. To demonstrate the feasibility of using trehalose mediated lipid array generation for SPR imaging, a number of assays were conducted using a home-built SPRi instrument in the Kretschmann configuration.<sup>26</sup>

First, membrane confinement was investigated in order to establish that supported membranes remain localized to the area of deposition during and after the hydration-fusion step. An array pattern on a planar SiO<sub>2</sub> covered gold surface was hand spotted with vesicles suspended in trehalose, and desiccated, and SPR difference images were taken before, during, and after hydration in the flow cell environment (Figure 4a). The initial SPR difference image of the as deposited spots was recorded at a lower angle allowing SPR resonance in air compared to the rehydrated substrate difference images that were imaged in buffer. Post-hydration and under a maintained flow rate of 6 mL/h, the resulting SLBs stay confined to their areas of deposition and fusion, as seen in Figure 4a. The observed spatial confinement is in agreement with the previous study involving fluorescence,<sup>16</sup> but extends this to a laminar flow regime, providing an additional measure of assurance that there is no cross talk between adjacent spots. During the vitrification of trehalose and removal of water from the

environment, embedded SUVs undergo significant shape deformation, which is restored once water is added back to the system.<sup>16</sup> This shape deformation likely plays an important role in determining minimum distances for eliminating cross talk of adjacent spots, as this may cause the bulk deposited vesicle surface area to laterally stretch from the arrayed spot. Nevertheless, this does not seem to have any negative impact on results, even with spacing <100 μm.<sup>16</sup>

This was further explored by spotting a microarray substrate for biological recognition, that on hydration resulted in 800 × 800 μm POPC membranes containing either GM1, GM2, GM3, or no receptors, as a negative control. Previous work has shown that cholera toxin has a very low affinity toward GM2 and GM3 compared to GM1 and no affinity toward POPC alone.<sup>10</sup> Figure 4b shows an SPR difference image comparing bare silica and devitrified SLB array spots on a patterned SPR imaging array substrate, where the high contrast between each row together with the sharp boundaries is indicative of bilayer formation in orderly rows, without migration of elements into adjacent ones. Assaying the array on the SPR imager with various concentrations of cholera toxin in the range 120–600 nM revealed that only SLBs containing the GM1 receptor yielded measurable signals, while in array elements containing GM2 and GM3 the signal remained at baseline values. This clearly demonstrates that vesicles released from trehalose during the devitrification and bilayer fusion processes do not mix with those in adjacent array spots, resulting in a lack of cross talk between array elements. To the best of our knowledge, this represents the first direct assaying of these three receptors side by side within their natural lipid environments in a microarray format.

**Beyond SLBs: Trehalose-Mediated Hybrid Bilayer Membranes.** Hybrid bilayer membranes (HBMs) are a classic model of biomimetic systems<sup>22</sup> and an active research area for investigating biophysical processes.<sup>39,40</sup> In hybrid membranes, the lower leaflet of the bilayer membrane is composed of hydrophobic molecules covalently bound to the substrate

surface, whereas the upper leaflet is composed of phospholipids. The rigidity of the hydrophobic lower leaflet reduces the lateral mobility of the lipid leaflet; however, their high mechanical stability and ease of integration with many optical and electrochemical techniques are heavily exploited in current sensor design. Since the formation of HBMs essentially follows similar steps as the formation of SLBs, we demonstrate that our trehalose assisted methodology for on-demand lipid membrane generation in SPRi analysis is also applicable toward HBMs (Figure 5a). Fluorescence images (Figure S5, Supporting Information) show that the fused phospholipids uniformly, across all observed length scales, cover the hydrophobic octadecanethiol-modified gold surface. FRAP analysis of the lipids mobility in the hybrid bilayer showed that these are far less mobile than both traditional and trehalose mediated SLBs, with a diffusion coefficient of  $0.48 \mu\text{m}^2/\text{s}$  and mobile fraction of 51%. This is to be expected, as the affinity of phospholipid tails for the underlying hydrophobic monolayer is much stronger than the hydrophilic reactions supporting lipid bilayers,<sup>41</sup> limiting lateral movement of these lipids. SPRi assaying of the system followed the same procedures as for the SLB system. Formed HBMs remain confined under buffer flow to locations where the arrays were originally spotted and vitrified, as seen in the SPR difference image (Figure 5b). In addition, the hydrophobic SPR substrate was spotted with arrays of SUVs incorporating GM1, GM2, GM3, or no receptors. The sensorgrams (Figure 5c) during the injection of 120 nM cholera toxin across this array confirm that binding only occurs to the HBMs containing GM1. These results align well with those obtained for the hydrophilic SLB arrays and demonstrate that the methods developed in this work are applicable to various surfaces and membrane geometries.

## CONCLUSIONS

The combination of trehalose-mediated phospholipid vesicle deposition and their on-demand fusion into SLBs combined with SPR spectroscopy and imaging is an efficient, powerful, and easily scalable tool for label-free assaying of molecular interactions with SLBs. Supported lipid bilayers produced by this method are of high quality and are nearly indistinguishable from those generated by traditional vesicle fusion methods. Fluorescence microscopy and FRAP analysis showed that the membranes on our engineered SPR chips are uniform and exhibit high lateral mobility, similar to native membrane environments. SPR spectroscopic studies show the bilayers from trehalose released vesicles are equivalent to conventionally generated bilayers in terms of effective refractive index values, and, hence, membrane geometry and packing density. Incorporation of the GM1 receptor into these systems resulted in binding of its natural ligand, cholera toxin, similar to that for traditionally prepared membranes. Furthermore, deposited lipids were stored in their vitrified state for up to one month while maintaining excellent ligand binding affinity upon hydration. Newly formed membranes stayed confined to their deposited spots upon hydration on both hydrophilic and hydrophobic SPR substrates, without crosstalk, which allows for the high-throughput screening of multiple SLBs with varying constituents. Taken together, these results represent a substantial step forward in the advancement of label-free lipid membrane arrays. We expect the methods reported here to inspire more widespread adaption of supported membrane systems, as the on-demand and label-free nature of this scheme is highly efficient, scalable, and convenient. Current work is

focusing on exploring the limits of printing density with a variety of deposition methods, as well as printing arrays of higher complexity that are true to their *in vivo* counterparts and suitable for clinical diagnostics.

## ASSOCIATED CONTENT

### Supporting Information

Gold well SPR array substrate fabrication, FRAP recovery curves, additional SPR sensorgrams, and FRAP data for HBMs in Figures S1–S5. The Supporting Information is available free of charge on the ACS Publications website at DOI: 10.1021/acsami.5b03809.

## AUTHOR INFORMATION

### Corresponding Authors

\*E-mail: [tewilkop@ucdavis.edu](mailto:tewilkop@ucdavis.edu).

\*E-mail: [quan.cheng@ucr.edu](mailto:quan.cheng@ucr.edu).

### Notes

The authors declare no competing financial interest.

## ACKNOWLEDGMENTS

The authors thank Dr. David Carter from UCR Institute for Integrative Genome Biology for training and assistance with the CLSM. We acknowledge support from the National Science Foundation (CHE-1413449). S.S.H. was supported by an NIEHS T32 training grant (T32-ES018827).

## REFERENCES

- (1) van Meer, G.; Voelker, D. R.; Feigenson, G. W. Membrane Lipids: Where They Are and How They Behave. *Nat. Rev. Mol. Cell Biol.* **2008**, *9*, 112–124.
- (2) Cuatrecasas, P. Membrane Receptors. *Annu. Rev. Biochem.* **1974**, *43*, 169–214.
- (3) Brian, A. A.; McConnell, H. M. Allogeneic Stimulation of Cytotoxic T Cells by Supported Planar Membranes. *Proc. Natl. Acad. Sci. U. S. A.* **1984**, *81*, 6159–6163.
- (4) Phillips, K. S.; Cheng, Q. Microfluidic Immunoassay for Bacterial Toxins with Supported Phospholipid Bilayer Membranes on Poly-(Dimethylsiloxane). *Anal. Chem.* **2005**, *77*, 327–334.
- (5) Costello, D. A.; Hsia, C. Y.; Millet, J. K.; Porri, T.; Daniel, S. Membrane Fusion-Competent Virus-Like Proteoliposomes and Proteinaceous Supported Bilayers Made Directly from Cell Plasma Membranes. *Langmuir* **2013**, *29*, 6409–6419.
- (6) Costello, D. A.; Millet, J. K.; Hsia, C. Y.; Whittaker, G. R.; Daniel, S. Single Particle Assay of Coronavirus Membrane Fusion with Proteinaceous Receptor-Embedded Supported Bilayers. *Biomaterials* **2013**, *34*, 7895–7904.
- (7) Grakoui, A.; Bromley, S. K.; Sumen, C.; Davis, M. M.; Shaw, A. S.; Allen, P. M.; Dustin, M. L. The Immunological Synapse: A Molecular Machine Controlling T Cell Activation. *Science* **1999**, *285*, 221–227.
- (8) Mossman, K. D.; Campi, G.; Groves, J. T.; Dustin, M. L. Altered TCR Signaling from Geometrically Repatterned Immunological Synapses. *Science* **2005**, *310*, 1191–1193.
- (9) Ghang, Y. J.; Schramm, M. P.; Zhang, F.; Acey, R. A.; David, C. N.; Wilson, E. H.; Wang, Y. S.; Cheng, Q.; Hooley, R. J. Selective Cavitand-Mediated Endocytosis of Targeted Imaging Agents into Live Cells. *J. Am. Chem. Soc.* **2013**, *135*, 7090–7093.
- (10) Kuziemko, G. M.; Stroh, M.; Stevens, R. C. Cholera Toxin Binding Affinity and Specificity for Gangliosides Determined by Surface Plasmon Resonance. *Biochemistry* **1996**, *35*, 6375–6384.
- (11) Cornell, B. A.; BraachMaksyvtis, V. L. B.; King, L. G.; Osman, P. D. J.; Raguse, B.; Wiczorek, L.; Pace, R. J. A Biosensor That Uses Ion-Channel Switches. *Nature* **1997**, *387*, 580–583.
- (12) Bayley, H.; Cremer, P. S. Stochastic Sensors Inspired by Biology. *Nature* **2001**, *413*, 226–230.



- (13) Groves, J. T.; Boxer, S. G. Micropattern Formation in Supported Lipid Membranes. *Acc. Chem. Res.* **2002**, *35*, 149–157.
- (14) Kaufmann, S.; Sobek, J.; Textor, M.; Reimhult, E. Supported Lipid Bilayer Microarrays Created by Non-Contact Printing. *Lab Chip* **2011**, *11*, 2403–2410.
- (15) Phillips, K. S.; Wilkop, T.; Wu, J. J.; Al-Kaysi, R. O.; Cheng, Q. Surface Plasmon Resonance Imaging Analysis of Protein-Receptor Binding in Supported Membrane Arrays on Gold Substrates with Calcinated Silicate Films. *J. Am. Chem. Soc.* **2006**, *128*, 9590–9591.
- (16) Wilkop, T. E.; Sanborn, J.; Oliver, A. E.; Hanson, J. M.; Parikh, A. N. On-Demand Self-Assembly of Supported Membranes Using Sacrificial, Anhydrobiotic Sugar Coats. *J. Am. Chem. Soc.* **2014**, *136*, 60–63.
- (17) Crowe, J. H.; Hoekstra, F. A.; Crowe, L. M. Anhydrobiosis. *Annu. Rev. Physiol.* **1992**, *54*, 579–599.
- (18) Crowe, L. M.; Crowe, J. H. Stabilization of Dry Liposomes by Carbohydrates. *Dev. Biol. Stand.* **1992**, *74*, 285–294.
- (19) Homola, J.; Yee, S. S.; Gauglitz, G. Surface Plasmon Resonance Sensors: Review. *Sens. Actuators, B* **1999**, *54*, 3–15.
- (20) Homola, J. Surface Plasmon Resonance Sensors for Detection of Chemical and Biological Species. *Chem. Rev.* **2008**, *108*, 462–493.
- (21) Zhao, S. S.; Bukar, N.; Toulouse, J. L.; Pelechacz, D.; Robitaille, R.; Pelletier, J. N.; Masson, J. F. Miniature Multi-Channel SPR Instrument for Methotrexate Monitoring in Clinical Samples. *Biosens. Bioelectron.* **2015**, *64*, 664–670.
- (22) Plant, A. L. Supported Hybrid Bilayer Membranes as Rugged Cell Membrane Mimics. *Langmuir* **1999**, *15*, 5128–5135.
- (23) Phillips, K. S.; Han, J. H.; Martinez, M.; Wang, Z. Z.; Carter, D.; Cheng, Q. Nanoscale Classification of Gold Substrates for Surface Plasmon Resonance Analysis of Protein Toxins with Supported Lipid Membranes. *Anal. Chem.* **2006**, *78*, 596–603.
- (24) Abbas, A.; Linman, M. J.; Cheng, Q. A. Patterned Resonance Plasmonic Microarrays for High-Performance SPR Imaging. *Anal. Chem.* **2011**, *83*, 3147–3152.
- (25) Linman, M. J.; Abbas, A.; Roberts, C. C.; Cheng, Q. Etched Glass Microarrays with Differential Resonance for Enhanced Contrast and Sensitivity of Surface Plasmon Resonance Imaging Analysis. *Anal. Chem.* **2011**, *83*, 5936–5943.
- (26) Wilkop, T.; Wang, Z. Z.; Cheng, Q. Analysis of Mu-Contact Printed Protein Patterns by SPR Imaging with a Led Light Source. *Langmuir* **2004**, *20*, 11141–11148.
- (27) Axelrod, D.; Koppel, D. E.; Schlessinger, J.; Elson, E.; Webb, W. W. Mobility Measurement by Analysis of Fluorescence Photobleaching Recovery Kinetics. *Biophys. J.* **1976**, *16*, 1055–1069.
- (28) Soumpasis, D. M. Theoretical-Analysis of Fluorescence Photobleaching Recovery Experiments. *Biophys. J.* **1983**, *41*, 95–97.
- (29) Stelzle, M.; Miehlich, R.; Sackmann, E. 2-Dimensional Microelectrophoresis in Supported Lipid Bilayers. *Biophys. J.* **1992**, *63*, 1346–1354.
- (30) Linman, M. J.; Culver, S. P.; Cheng, Q. Fabrication of Fracture-Free Nanoglassified Substrates by Layer-by-Layer Deposition with a Paint Gun Technique for Real-Time Monitoring of Protein-Lipid Interactions. *Langmuir* **2009**, *25*, 3075–3082.
- (31) Szunerits, S.; Coffinier, Y.; Janel, S.; Boukherroub, R. Stability of the Gold/Silica Thin Film Interface: Electrochemical and Surface Plasmon Resonance Studies. *Langmuir* **2006**, *22*, 10716–10722.
- (32) Szunerits, S.; Boukherroub, R. Electrochemical Investigation of Gold/Silica Thin Film Interfaces for Electrochemical Surface Plasmon Resonance Studies. *Electrochem. Commun.* **2006**, *8*, 439–444.
- (33) Kambhampati, D. K.; Jakob, T. A. M.; Robertson, J. W.; Cai, M.; Pemberton, J. E.; Knoll, W. Novel Silicon Dioxide Sol-Gel Films for Potential Sensor Applications: A Surface Plasmon Resonance Study. *Langmuir* **2001**, *17*, 1169–1175.
- (34) Chen, C.-Y.; Hinman, S. S.; Duan, J.; Cheng, Q. Nanoglassified, Optically-Active Monolayer Films of Gold Nanoparticles for in Situ Orthogonal Detection by Localized Surface Plasmon Resonance and Surface-Assisted Laser Desorption/Ionization-MS. *Anal. Chem.* **2014**, *86*, 11942–11945.
- (35) Ay, F.; Aydinli, A. Comparative Investigation of Hydrogen Bonding in Silicon Based PECVD Grown Dielectrics for Optical Waveguides. *Opt. Mater.* **2004**, *26*, 33–46.
- (36) Reits, E. A. J.; Neeffjes, J. J. From Fixed to FRAP: Measuring Protein Mobility and Activity in Living Cells. *Nat. Cell Biol.* **2001**, *3*, E145–E147.
- (37) Sprague, B. L.; McNally, J. G. FRAP Analysis of Binding: Proper and Fitting. *Trends Cell Biol.* **2005**, *15*, 84–91.
- (38) Taylor, J. D.; Phillips, K. S.; Cheng, Q. Microfluidic Fabrication of Addressable Tethered Lipid Bilayer Arrays and Optimization Using SPR with Silane-Derivatized Nanoglassy Substrates. *Lab Chip* **2007**, *7*, 927–930.
- (39) Ma, W.; Ying, Y. L.; Qin, L. X.; Gu, Z.; Zhou, H.; Li, D. W.; Sutherland, T. C.; Chen, H. Y.; Long, Y. T. Investigating Electron-Transfer Processes Using a Biomimetic Hybrid Bilayer Membrane System. *Nat. Protoc.* **2013**, *8*, 439–450.
- (40) Tse, E. C. M.; Barile, C. J.; Gewargis, J. P.; Li, Y.; Zimmerman, S. C.; Gewirth, A. A. Anion Transport through Lipids in a Hybrid Bilayer Membrane. *Anal. Chem.* **2015**, *87*, 2403–2409.
- (41) Castellana, E. T.; Cremer, P. S. Solid Supported Lipid Bilayers: From Biophysical Studies to Sensor Design. *Surf. Sci. Rep.* **2006**, *61*, 429–444.